ISTITUTO NAZIONALE DI FISICA NUCLEARE

Sezione di Napoli

INFN/AE-92/18
1 Giugno 1992

F. D'Aquino, G. Iaselli, S. Nuzzo, A. Ranieri, F. Romano, P. Pistilli, M. Ambrosio, G.C. Barbarino, B. Bartoli, D. Campana, M. Iacovacci, F. Guarino, G. Osteria, V. Silvestrini, S. Del Sordo, L. Scarsi, G. Bressi, A. Lanza, M. Bonori, A. Nigro, R. Cardarelli, R. Santonico, M. Guida, G.Marini:

REJECTION POWER OF A HORIZONTAL RPC TELESCOPE FOR LEFT AND RIGHT COMING COSMIC MUONS

Servizio Documentazione
dei Laboratori Nazionali di Frascati

INFN - Istituto Nazionale di Fisica Nucleare
Sezione di Napoli

INFN/AE-92/18
1 Giugno 1992

Rejection power of a horizontal RPC telescope for left and right coming cosmic muons

MINI Collaboration

F.D'Aquino, G.Iaselli, S.Nuzzo, A.Ranieri, F.Romano
INFN-Università di Bari I-70126 Bari, Italy.

P.Pistilli
INFN-Università di Lecce I-73100 Lecce, Italy.

M.Ambrosio, G.C.Barbarino, B.Bartoli, D.Campana, M.Iacovacci, F.Guarino, G.Osteria, V.Silvestrini
INFN-Università di Napoli I-80125 Napoli, Italy

S.Del Sordo, L.Scarsi
IFCAI(CNR)-Università di Palermo I-90100 Palermo,Italy

G.Bressi, A.Lanza
INFN-Università di Pavia I-27100 Pavia, Italy

M.Bonori, A.Nigro
INFN-Università di Roma I I-00115 Roma, Italy

R.Cardarelli, R.Santonico
INFN-Università di Roma II I-00173 Roma TOV, Italy

M.Guida, G.Marini
INFN-Università di Salerno I-84081 Salerno, Italy

Abstract

The possibility of performing a neutrino astronomy by means of a detector above the ground depends critically on the feasibility of a rejection power on the order of 10^{11} required to discriminate the enormous background of cosmic downward going muons from the signal of upward going muons produced by neutrinos. In order to check whether and how this rejection is obtainable, we have built in the Physics Department of the University of Bari a horizontal cosmic muon telescope (MINI) instrumented with Resistive Plate Counters. By performing time of flight measurements, we have estimated the rejection power of our telescope for left and right coming cosmic muons. The rejection dependence on a few fundamental parameters like minimum number of points per track, telescope length, RPC time resolution and on trigger configuration has been investigated.

Introduction

One way of identifying astrophysical sources of high energy neutrinos relies on the possibility of detecting upward going muons produced by charged current interactions of these neutrinos in the rock below the telescope. The main requirements of such a detector are : a) an excellent angular resolution, in fact the muon direction lies within 1° with respect to the direction of the parent neutrino; b) a high capability of discriminating against the background muons which are produced by cosmic ray interactions in the atmosphere. Two techniques are currently employed: the first exploits the directionality of the Cerenkov radiation created in a large body of water by fast muons (IMB [1] and KAMIOKANDE [2]); the second one is based on the time of flight measurement of crossing muons performed by two or three layers of scintillation counters coupled to a tracking device (BST [3] and MACRO [4]). Such telescopes are located in underground sites to lower the background from cosmic ray muons to a level of about 10^5-10^6 times the expected signal, therefore they require a rejection power of the order of 10^6-10^7 to operate successfully.

On the other hand the present estimates of neutrino fluxes from candidate sources (compact sources such as X-ray binaries in our galaxy or active galactic nuclei) indicate that very large sensitive areas, larger than 10^4 m^2, may be required to detect the signals [5]. Such large area apparatus cannot longer be located underground because of the severe space limitations imposed by any underground laboratory.

A recently proposed approach [6] for constructing above-ground neutrino detectors suggest to use a stack of Resistive Plate Counters (RPCs) interleaved with thick concrete layers. Since RPCs are able to provide a very high time resolution, the time of flight technique could discriminate between upward and downward going muons at the level required by a surface neutrino detector. Such an apparatus can be large and can be expanded as necessary to perform searches for astronomical point sources of multi-GeV neutrinos.

Any signal would be observed in the presence of three forms of background. One background is due to upward going muons produced by the atmospheric neutrinos. These muons are an unavoidable background which depends weakly on the zenith angle. With a muon threshold of 2 GeV, it has been estimated to be near $3.5 \cdot 10^{-13}$ cm^{-2} s^{-1} sr^{-1} [7]. The effect of this background on the sensitivity of a neutrino point source detector is greatly reduced by increasing the angular resolution of the detector. The background in a 1° radius angular region is only about 1 count/year in 10000 m^2 .

Another background is due to the muons backscattered in the ground around and below the detector. This flux has been calculated [8] and found to be a limiting factor only for directions within about 11° (24°) on the horizon for $E_\mu > 5$ (2) GeV; at higher elevation angles the backscattered muon flux is negligible when compared to the atmospheric neutrino background.

The last background source is instrumental in origin, arising from mistakenly reconstructed tracks: a downward going muon might be reconstructed and tagged as upward going. Due to the enormity of the cosmic ray muon flux, compared with the predicted signal flux, it appears that a surface neutrino apparatus requires a rejection power on the order of 10^{11} to reduce this background to levels such that they do not limit the sensitivity of the detector.

Since the first two sources of background can be kept under control, the possibility of performing neutrino astronomy on the surface is critically dependent on the feasibility of a rejection power of the order of 10^{11} .

To check whether this rejection is achievable, we have built at the Physics Department of the University of Bari a horizontal cosmic muon telescope instrumented with RPCs. By performing time of flight measurements we have studied the discrimination power between left and right coming cosmic muons achievable by MINI and more generally by a telescope of his type.

The MINI telescope

The RPC is a gas filled detector [9] consisting of two plane phenolic polymer electrodes (bakelite), 1 x 2 m^2 large, separated by a 2 mm gap filled with a gas mixture of Argon and Butane with a small amount of Freon. Depending on the gas mixture, a voltage of 8 to 10 kV is applied on the external face of the bakelite which is graphite coated. Typical signals from the RPC are 400 mV in amplitude and 10 ns long, with a 3 ns rise time. They can be collected by an external pick-up system like strips or pads of conducting material, the resistive electrodes being almost transparent to fast e.m. pulses. The discharge area is $\sim 10^{-1}$ cm^2.

The Fig.1 shows the MINI telescope [10] layout: ten RPC planes, (1+1) x 2 m^2 each, are separated by nine 1 m thick concrete absorbers corresponding to an energy threshold of ~4 GeV for muons crossing the entire apparatus. The total length of the telescope is 11 m corresponding to an elevation angle on the horizon of about 10°. In our case the RPCs are operated with a gas mixture of 47% Argon, 50% Butane, 3% Freon. In the telescope are present two kinds of RPCs having bakelite resistivity respectively of 10^{10} $\Omega * cm$ (planes nr. 3,4,5,6,7,8) and 10^{11} $\Omega * cm$ (planes nr. 1,2,9,10). The applied voltage is 8.8 and a 9.4 kV respectively with typical currents of a few hundreds of μA for the first type and a few tens of μA for the second type. The RPC planes nr. 1, 2, 4, 5, 6, 7, 9 and 10 are equipped with 2 m long, 3 cm wide, horizontal (along the Y direction) pick-up strips, while planes nr. 3 and 8 have vertical (along the X direction) strips . The crossing point along the strip direction is obtained from the difference in time between the signal arrivals at the opposite ends of the strip. The time measurements are carried out by means of Lecroy 2228A TDC module operated at 0.25 ns/chan.. Each TDC channel serves the OR of the 64 strips of a RPC read on the same side. Fig. 2 shows a typical muon event as seen by MINI.

Data analysis

In one month of operation (1990) the telescope has collected more than 100.000 events with the trigger provided by the coincidence of the planes 1^{st} and 10^{th} and the majority of 3 among the central ones 4^{th}, 5^{th}, 6^{th} and 7^{th}.

In order to reject horizontal showers and to select muon events, we have selected as candidate muon events those having not more than 20 strips fired in 15 clusters (a cluster is a set of contiguous strips), then the candidate event was required to have at least 4 planes with only one strip fired. The muon track was reconstructed by a straight line fit both in X and Y view, and the candidate event was accepted only if χ^2_x/d.o.f. $\leq$ 3. and χ^2_y/d.o.f. $\leq$ 3. The time response of the chambers has been computed excluding one chamber at a time from the time sequence $t_1, t_2, ..., t_{10}$ of the track, then performing on the "reduced" time sequence a linear fit of time versus position where a loose cut was applied, χ^2_t/d.o.f. $\leq$ 10. Finally the delay time of the chamber under consideration was calculated with respect to its ideal time defined by the fit. The contamination of the selected sample due to fake muon events has been estimated to be less than .1%. The efficiency of each chamber was found to be contained in the range 88% to 96% as reported in Tab 1.

The crossing point along the strip is very well reconstructed. Fig. 3 shows the distribution of the difference between the X position reconstructed in the chamber 8 by means of the TDC information and the "true" one, defined by the fit in the XZ view using the strip information. Each strip has been calibrated separately and the time has been corrected for the calibration constant relative to the fired strip. The r.m.s. is 3.5 cm.

The Fig. 4 shows a typical RPC time response distribution (chamber 6); the chamber time resolutions go from 3 to 5 ns as shown in Tab. 1. The Fig. 5a reports the time response distribution of all the chambers as if they were crossed by a muon travelling at the speed of the light and proceeding from the 10^{th} to the 1^{st} chamber, the mean crossing times are defined by the telescope length assuming that the 1^{st} chamber is hit at time 0.0 ns. The distributions are normalized to 1.0 so that on the vertical axis we have the probability P(t) that the RPC response occurs at the time t after the hit.

Rejection power calculation

method

In order to estimate the rejection power we have to remark that the events we want to compute the probability are very rare so that a usual Monte Carlo estimate would imply almost infinite cpu time. Therefore we have chosen the technique of the "weighted" Monte Carlo.

We have to estimate how many times a muon travelling from the 10^{th} to the 1^{st} chamber with velocity β =v/c=+1 (c: light speed) is tagged as traveling from the 1^{st} to the 10^{th} chamber . The times at which each chamber is crossed by this muon are in a well defined sequence as shown in Fig. 5a.

As an event is defined by a sequence of observed times $t_1, t_2, ..., t_{10}$ a sequence was generated by taking each time t_i randomly and uniformly in -50. to 50. ns, provided the i^{th} chamber was fired according to the efficiencies reported in Tab. 1. The sequence of generated times was then submitted to a linear fit (time versus position) as for real events, and was accepted as an event if the χ^2/d.o.f. $\leq$ 3. The choice of this value comes from an optimization of the cut, a harder cut does not improve significantly the rejection factor, while the two cuts in χ^2/d.o.f., namely 3. and 2., correspond to a loss of 5% and 10% respectively of real events. This fit defined the β of the event. Once the sequence was accepted, its probability was computed as the product of the chamber time probabilities $\Pi_i P_i(t_i)$ with the index i going from 1 to 10 over all the fired chambers. At this point the event enters in a β histogram with a weight equal to $\Pi_i P_i(t_i)$. We generated $5 \cdot 10^8$ random sequences. The number of selected events is reported in Tab. 2. The weighted β distribution which comes out has a maximum around +1.0 as expected. After normalization of this distribution between -2.0 and +2.0, the inverse of the integral probability in the range -2.0 to +0.0 has been taken as the rejection power of the apparatus.

The unweighted β distribution is almost symmetric with respect to 0.0, with a light overabundance of events having β > 0. since, looking at Fig. 5a, the probability for high and negative response times of the chamber is zero.

In the rejection power estimation, the value of β has been limited to the range -2.0 to 2.0 because the real data β distribution shows that, even though there are events such that $|\beta| \geq 1.5$, the tail of β beyond $|\beta| \geq 2.0$ is practically zero,

In the computation, a constant probability was added to the probability resulting from the experimental time response distribution (see Fig. 5) only for times corresponding to a positive delay with respect to the ideal time. This constant probability that we refer to as constant probability tail has been estimated, chamber by chamber, by taking the events contained between the point where the experimental time response distribution ended to be continuous, or where the first hole appeared, and 50 ns. Typical value for the probability tail is the order of 10^{-5}/ns, the values for each chamber are reported in Tab. 1. Adding this constant probability corresponds to double the probability for long delay time response.

results

We have studied the rejection as function of the χ^2/d.o.f. cut, the minimum number of points per track, the trigger and the telescope lenght.

The Fig. 6 shows the behaviour of the rejection as function of the minimum number of points per track, npt_{min} /track, for two values of the probability tail, namely the estimation that comes from data and twice this value. The result is that the rejection depends very weakly on the tail estimation or even a factor of two error on the tail estimation does not change the result very much. Therefore the sensitivity of the rejection estimation to the tail estimation is weak when compared to other dependences.

The Fig. 7 shows the rejection still as function of npt_{min} /track for different trigger configurations that correspond to different minimun lever arms, la_{min}, of the time fit expressed in number of chambers, namely la_{min}=10, la_{min}=9 and la_{min}=8. We note that la_{min}=10 corresponds to our trigger. The effect of the trigger is evident at npt_{min} /track ≥5 and disappears at npt_{min} /track ≥ 8.

In Fig. 8 the rejection is reported for different telescope lengths. The dependence here is very strong as more as npt_{min} /track increases. Actually increasing the telescope length corresponds to better resolve from each other the curves of response time of the chambers what implies that longer times on the tails are needed to inverte the sign of β, but longer times correspond to lower probabilities so this strong dependence is explained. An estimation of the errors has been performed by looking for the same point at many estimations of it done in a few subsample of the total sample. The result is that half an order of magnitude is a good error estimate for the points relative to L=11m, instead between half to one order of magnitude error can be attributed to the points belonging to L=15.5 m and to L=20 m.

Since the RPC time resolution reported in literature is ≤ 2. ns [9], in order to investigate the dependence of our results upon it, we have simulated a set of distributions with a time resolution a factor two better ($\sigma=\sigma_{exp}/2$). This has been done summing the bin contents in Fig. 5a two by two, or rebinning at 2 ns, then rescaling the bin width from 2 to 1 ns, as shown in Fig. 5b. The constant tail, for each chamber, has been taken as twice the value reported in Tab.1. The rejection power has been computed for la_{min} =10 and L=11m, the result is in Fig. 9. The statistics is in this case of $3.5*10^9$ generated sequences and the error that can be associated to the points is half an order of magnitude. Being the behaviour of the rejection, as function of npt_{min} /track, almost linear in log scale, this implies that we are in a situation where adding a point to the track results in improving the rejection by an almost constant factor 10^n that, from the figure, can be taken as 10^2.

In all figures, it comes out that the dependence on the number of points per track is strong. This means that efficiencies are important, but one has to keep in mind that efficiency values higher than 95% are unrealistic for large RPC production. Considering that our trigger imposes la_{min} =10 and npt_{min} /track= 5, looking in Fig. 7 at the line corresponding to L=11m we can say our present rejection with MINI to be around 10^6. Nevertheless requiring at least 8 points per track, what select the 65% of the events, the rejection is better than 10^8.

Conclusions

A telescope like MINI provided with 2 ns time resolution RPCs would reach a rejection of 10^{11} by simply requiring at least 6 points per track. If, like in our case, the chambers have a worst time resolution by a factor two, then a longer telescope, 16 m, is needed and at least 8 points per track are needed to reach 10^{11} with a 35% loss of statistics. Otherwise, keeping the length at 11 m, the number of chambers has to be increased so to have 10 points per track in an high percentage of events.

Acknowledgements

We would like to thank J.W. Elbert for stimulating discussions and useful suggestions, B. D'Ettorre Piazzoli for critically reading this text and suggesting corrections to it, G. Auriemma and S. Natali for their support to this work.

References

[1] R. M. Bionta et al., Phys. Rev. Lett. **58**, 1490 (1987);
R. C. Svoboda et al., Ap. J., 315 (1987);
R. Becker-Szendy et al., 25th Int. Conf. on High Energy Physics, Singapore, Aug 2-8, 1990 .

[2] K. S. Hirata et al., Phys. Rev. Lett. **58**, 1494 (1987);
K. S. Hirata et al., Phys. Rev. Lett. **63**, 16 (1989);
K. S. Hirata et al., Phys. Rev. Lett. **65**, 1297 (1990);
K. S. Hirata et al., Phys. Rev. Lett. **66**, 9 (1991).

[3] E. N. Alexeev et al., ZhETF Lett. **45**, 461 (1987), also in JTEP Lett. **45**, 589 (1987);

[4] G. Battistoni et al., Nucl. Inst. Meth. **A270**, 185 (1988);
M. Calicchio et al., Nucl. Inst. Meth. **A264**, 18 (1988);
De Marzo et al., Nuovo Cimento **9C**, 281 (1986).

[5] V.S. Berezinsky, Proc. of the Third International Workshop on Neutrino Telescopes, edited by M. Baldo-Ceolin, Venice, 1991, p. 125 .

[6] P.Pistilli et al., Proc. of the International Workshop on Neutrino Telescopes, edited by M. Baldo-Ceolin, Venice, 1988, p. 334 ;
R. Santonico, Proc. of the International Workshop on Neutrino Telescopes, edited by M. Baldo-Ceolin, Venice, 1988, p. 353 ;
P. Pistilli, Proc. of Third the International Workshop on Neutrino Telescopes, edited by M. Baldo-Ceolin, Venice, 1991, p. 379.

[7] T.K. Gaisser and Todor Stanev, Phys. Rev. **D31**, 2770 (1985).

[8] J. Elbert, M. Iacovacci and V. Silvestrini, Europhys. Lett. **14** (2),181 (1991).

[9] R. Santonico and R. Cardarelli, Nucl. Instr. Meth. **187**, 377 (1981);
R. Cardarelli et al., Nucl. Instr. Meth. **A236** , 20 (1988).

[10] M. Ambrosio et al., Proc. of the Second International Workshop on Neutrino Telescopes, edited by M. Baldo-Ceolin, Venice, 1990, p. 219;
F. Romano et al., Proc. of the Vulcano Workshop 1990 - Frontier Objects in Astrophysics and Particle Physics, edited by F. Giovannelli and G. Mannocchi, Vulcano, 1990, p. 337;
R.Santonico et al., Nuclear Physics B (Proc. Suppl.) **14B**, 459 (1990);
M. Iacovacci et al., Proc. of the Third International Workshop on Neutrino *Telescopes, edited by M. Baldo-Ceolin, Venice, 1991, p 357.*

Tables

Tab. 1 Efficiency, time resolution and constant probability tail for each chamber. For meaning of constant probability tail see text.

Tab. 2 Number of selected events out of the $5*10^8$ ($3.5*10^9$ last row) trials according to the used cuts (see the text for the parameter meaning and explanations).

Figures

Fig.1 The MINI telescope.
Fig.2 Typical muon event as seen by MINI (the figure is not in scale).
Fig.3 Spatial resolution with TDC information.
Fig.4 Typical time response distribution.
Fig.5 a) Time response distributions of all the chambers; b) Simulated time response distributions with a better resolution : $\sigma=\sigma_{exp}/2$. The distributions include the contribution of a constant probability tail which has been added to the experimental probability and which is represented by the dashed line in each histogram .
Fig.6 The rejection as function of the minimum point number per track for two values of the probability tail.
Fig.7 The trigger effect.
Fig.8 The rejection for different telescope length.
Fig.9 The rejection with a better time resolution: $\sigma=\sigma_{exp}/2$.

TABLE 1

Chamber #	Efficiency (%)	Time resolution (ns)	Probability tail (10^{-5}/ns)
1	96	2.9	0.2
2	83	2.9	2.0
3	95	4.0	1.6
4	92	4.0	2.3
5	89	4.0	1.1
6	88	3.5	1.6
7	90	5.0	1.1
8	88	5.0	0.8
9	90	2.9	0.6
10	96	2.9	0.2

TABLE 2

	npt_{min}/track					
events	5	6	7	8	9	10
L=11 m, la_{min}=8	62812	58732	48047	30324		
L=11 m, la_{min}=9	56579	53651	45083	29454	12523	
L=11 m, la_{min}=10	46728	44581	38073	25758	11605	2446
L=16 m, la_{min}=10	10988	10015	7798	4635	1767	320
L=20 m, la_{min}=10	3774	3245	2293	1206	382	65
$\sigma(t) = \sigma_{exp}(t)/2$	8660	7019	4313	1998	490	51

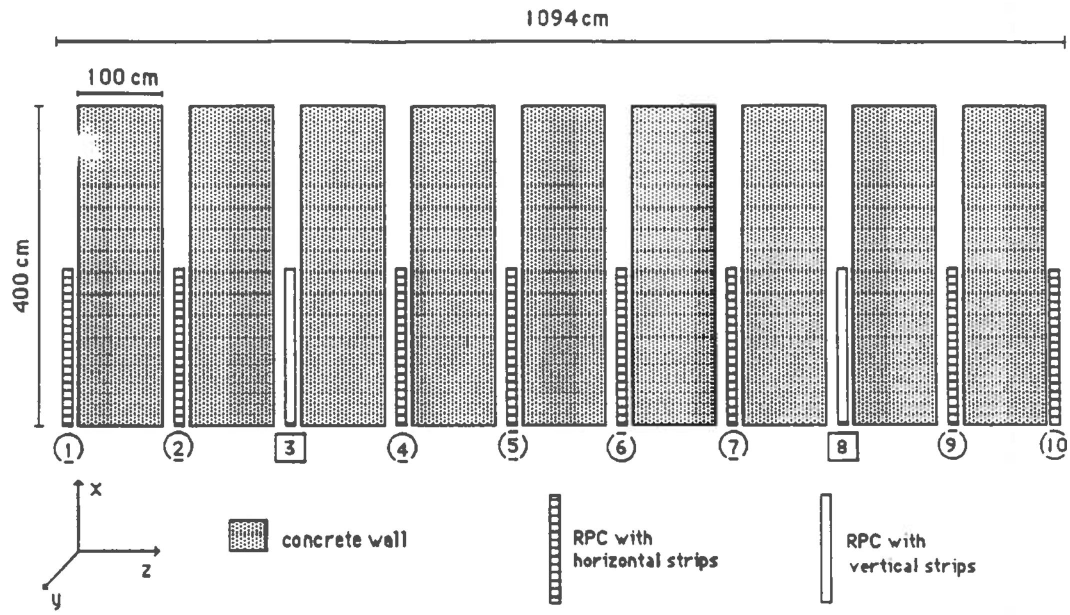
1094cm
100 cm
400 cm
1
2
3
4
5
6
7
8
9
10
x
z
y
concrete wall
RPC with
horizontal strips
RPC with
vertical strips

FIG. 1

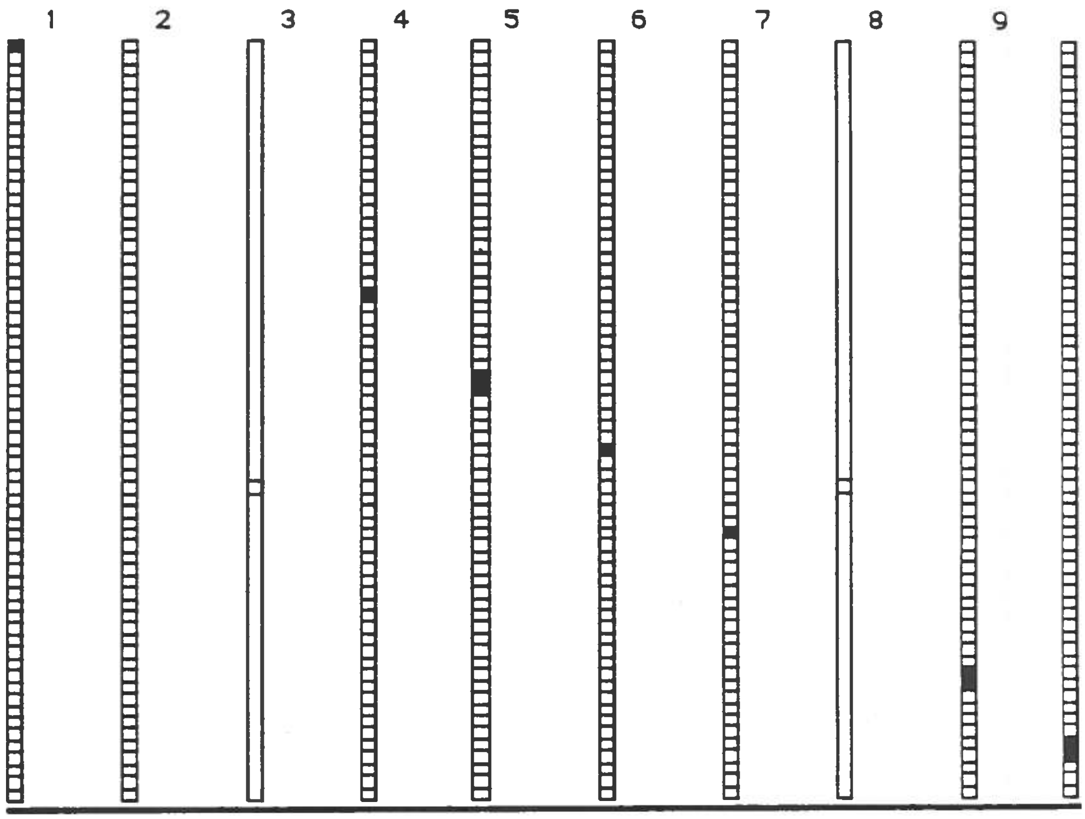
1
2
3
4
5
6
7
8
9

FIG. 2

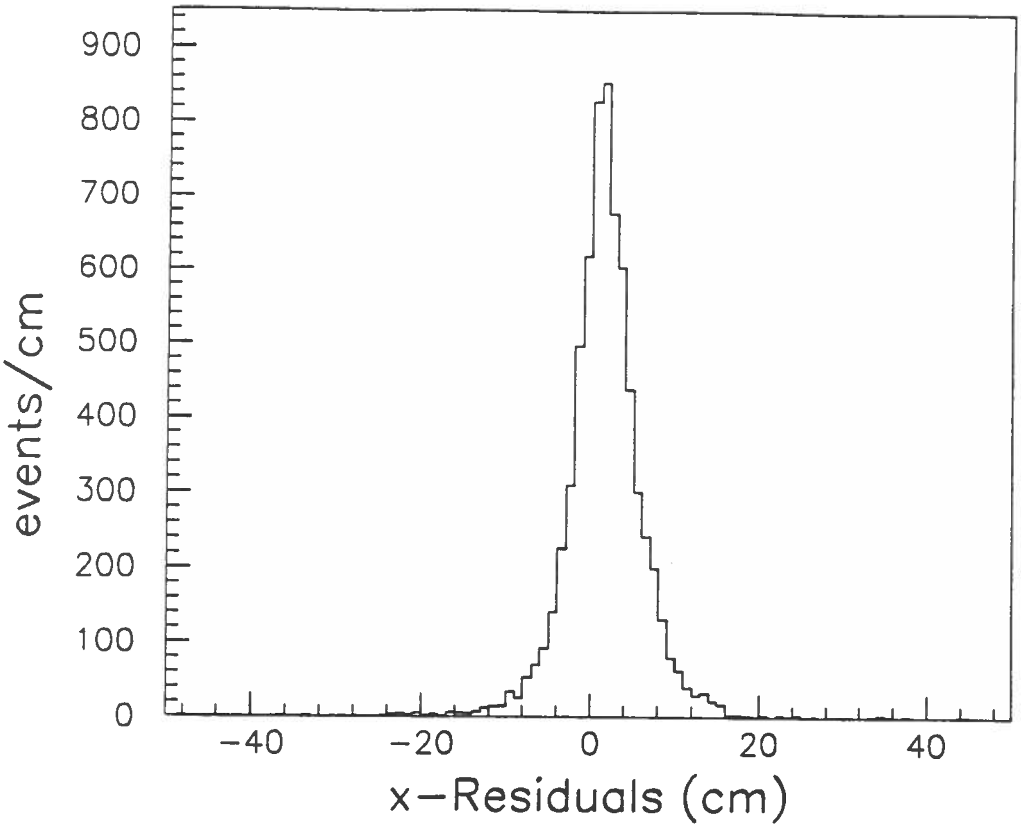

900
800
700
600
500
400
300
200
100
0
events/cm
-40
-20
0
20
40
x-Residuals (cm)

FIG. 3

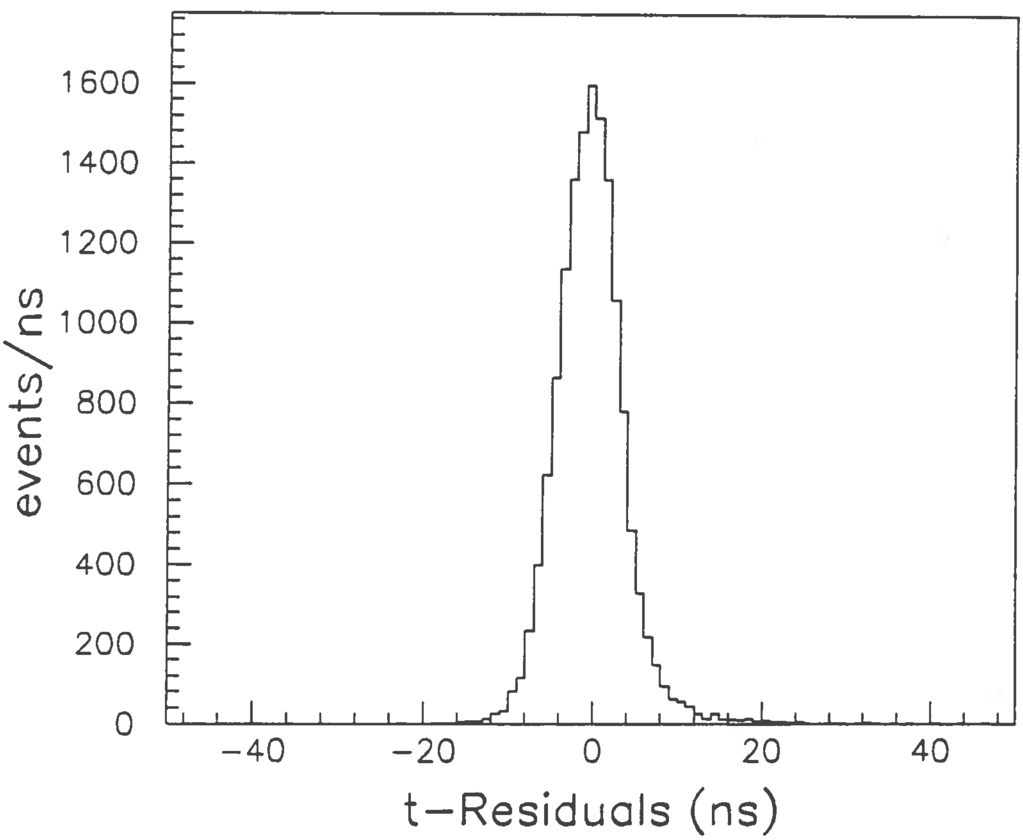

1600
1400
1200
1000
800
600
400
200
0
events/ns
-40
-20
0
20
40
t-Residuals (ns)

FIG. 4

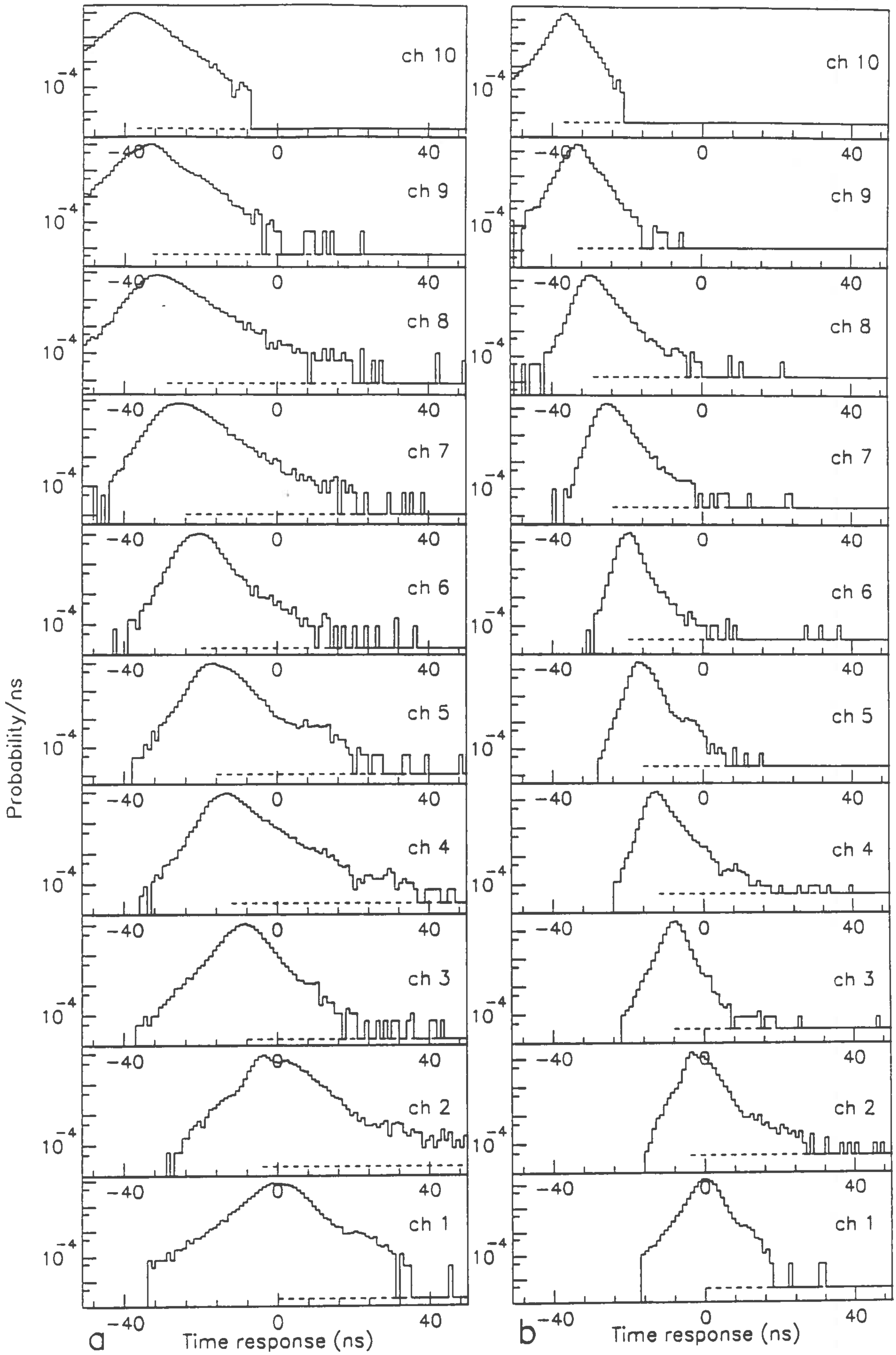
ch 10
ch 9
ch 8
ch 7
ch 6
ch 5
ch 4
ch 3
ch 2
ch 1
Probability/ns
a
b
Time response (ns)
-40
0
40

FIG. 5

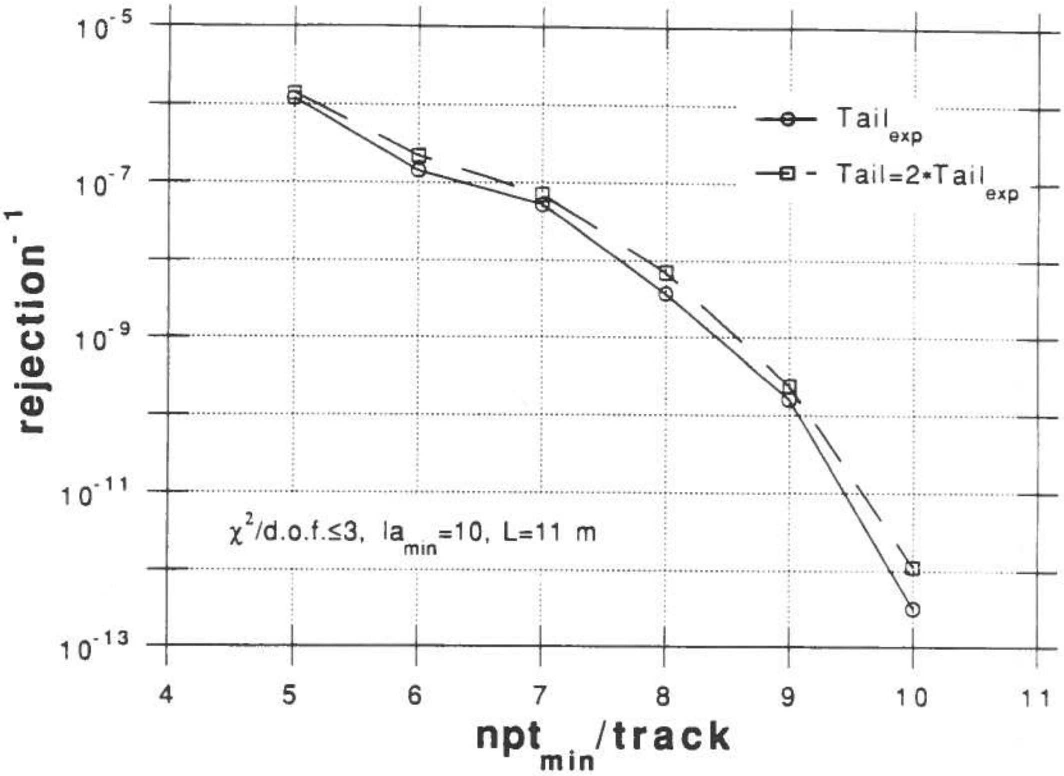

rejection⁻¹
10⁻⁵
10⁻⁷
10⁻⁹
10⁻¹¹
10⁻¹³
4
5
6
7
8
9
10
11
npt_min/track
Tail_exp
Tail=2*Tail_exp
χ²/d.o.f.≤3, la_min=10, L=11 m

FIG. 6

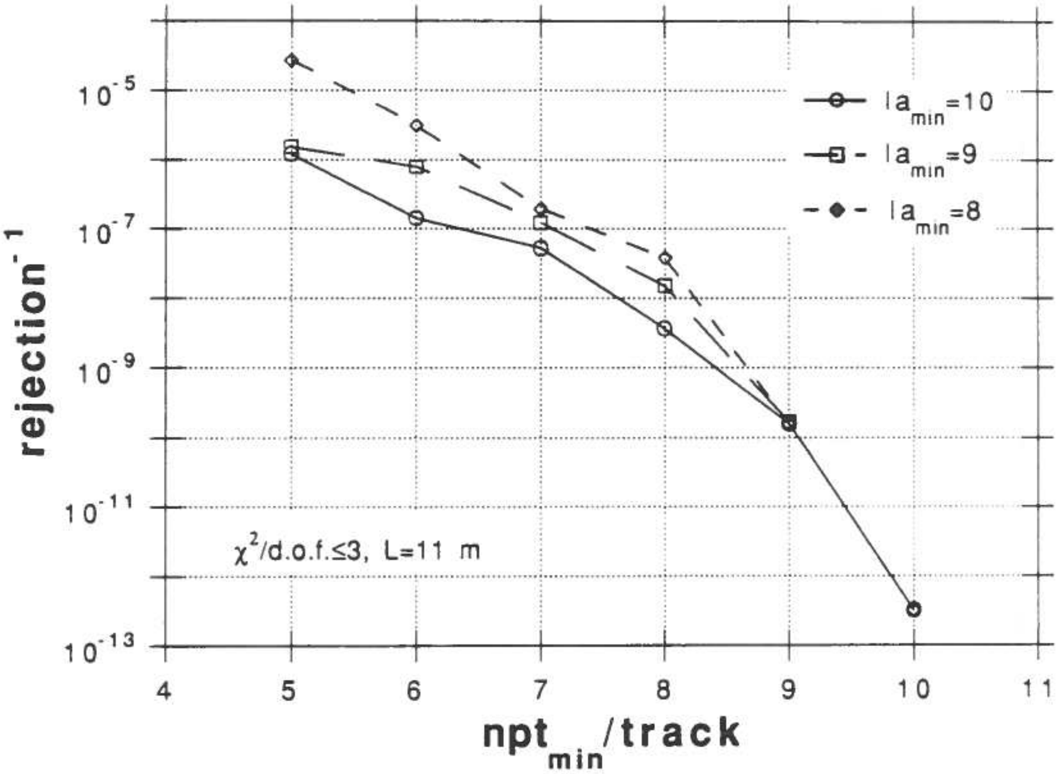

rejection⁻¹
10⁻⁵
10⁻⁷
10⁻⁹
10⁻¹¹
10⁻¹³
4
5
6
7
8
9
10
11
npt_min/track
la_min=10
la_min=9
la_min=8
χ²/d.o.f.≤3, L=11 m

FIG. 7

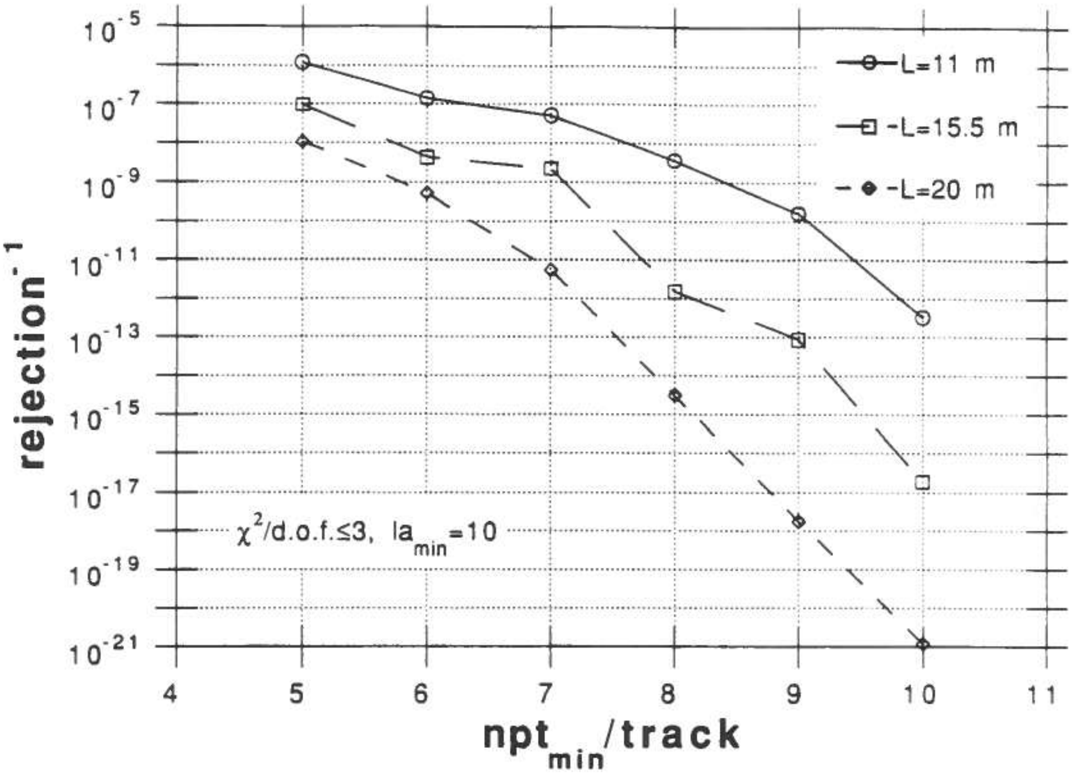

L=11 m
L=15.5 m
L=20 m
χ^2/d.o.f.≤3, la_{min}=10
rejection^{-1}
npt_{min}/track

FIG. 8

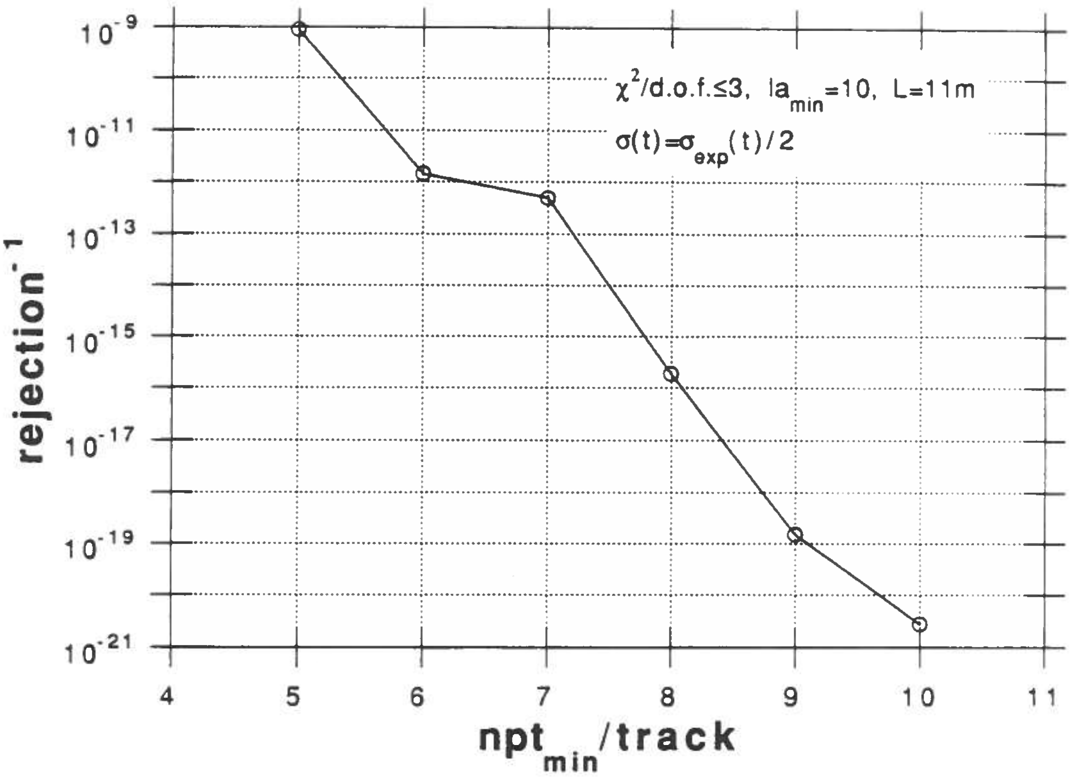

χ^2/d.o.f.≤3, la_{min}=10, L=11m
$\sigma(t)=\sigma_{exp}(t)/2$
rejection^{-1}
npt_{min}/track

FIG. 9